



# Morphological Properties of Gastropod Shells in a Warmer and More Acidic Future Ocean Using 3D Micro-Computed Tomography

Eva Chatzinikolaou<sup>1\*</sup>, Kleoniki Keklikoglou<sup>1,2</sup> and Panos Grigoriou<sup>3</sup>

<sup>1</sup> Hellenic Centre for Marine Research (HCMR), Institute of Marine Biology, Biotechnology and Aquaculture (IMBBC), Heraklion, Crete, Greece, <sup>2</sup> Biology Department, University of Crete, Heraklion, Crete, Greece, <sup>3</sup> Hellenic Centre for Marine Research (HCMR), CretAquarium, Heraklion, Crete, Greece

The increased absorption of atmospheric CO<sub>2</sub> by the ocean reduces pH and affects the carbonate chemistry of seawater, thus interfering with the shell formation processes of marine calcifiers. The present study aims to examine the effects of ocean acidification and warming on the shell morphological properties of two intertidal gastropod species, *Nassarius nitidus* and *Columbella rustica*. The experimental treatments lasted for 3 months and combined a temperature increase of 3°C and a pH reduction of 0.3 units. The selected treatments reflected the high emissions (RCP 8.5) “business as usual” scenario of the Intergovernmental Panel on Climate Change models for eastern Mediterranean. The morphological and architectural properties of the shell, such as density, thickness and porosity were examined using 3D micro-computed tomography, which is a technique giving the advantage of calculating values for the total shell (not only at specific points) and at the same time leaving the shells intact. *Nassarius nitidus* had a lower shell density and thickness and a higher porosity when the pH was reduced at ambient temperature, but the combination of reduced pH and increased temperature did not have a noticeable effect in comparison to the control. The shell of *Columbella rustica* was less dense, thinner and more porous under acidic and warm conditions, but when the temperature was increased under ambient pH the shells were thicker and denser than the control. Under low pH and ambient temperature, shells showed no differences compared to the control. The vulnerability of calcareous shells to ocean acidification and warming appears to be variable among species. Plasticity of shell building organisms as an acclimation action toward a continuously changing marine environment needs to be further investigated focusing on species or shell region specific adaptation mechanisms.

**Keywords:** climate change, ocean acidification, shell density, shell thickness, shell porosity, gastropod, micro-CT

## INTRODUCTION

The last three decades were the warmest period of the last 1,400 years in the Northern Hemisphere of the planet (IPCC, 2014). The upper 75 m of the sea surface have been experiencing strongest warming (0.11°C per decade) over the period 1971 to 2010 (IPCC, 2014). According to the IPCC (2014) high GHG emissions scenario (RCP8.5) the global mean surface temperature will

## OPEN ACCESS

### Edited by:

Jonathan Y. S. Leung,  
University of Adelaide, Australia

### Reviewed by:

Fiorella Prada,  
University of Bologna, Italy  
Kristina Barclay,  
University of Calgary, Canada

### \*Correspondence:

Eva Chatzinikolaou  
evachat@hcmr.gr

### Specialty section:

This article was submitted to  
*Global Change and the Future Ocean*,  
a section of the journal  
*Frontiers in Marine Science*

**Received:** 23 December 2020

**Accepted:** 30 March 2021

**Published:** 28 April 2021

### Citation:

Chatzinikolaou E, Keklikoglou K  
and Grigoriou P (2021) Morphological  
Properties of Gastropod Shells in a  
Warmer and More Acidic Future  
Ocean Using 3D Micro-Computed  
Tomography.  
*Front. Mar. Sci.* 8:645660.  
doi: 10.3389/fmars.2021.645660

be 1.4 - 2.6°C higher during the next 25-44 years. At the same time, the oceans have absorbed approximately 25% of all the CO<sub>2</sub> released into the atmosphere by humans since the start of the Industrial Revolution, which has resulted in a reduction of the ocean surface pH by 0.1 units (Orr et al., 2005; IPCC, 2014). The carbonates dissolved in seawater include biogenic magnesium calcites from coralline algae, aragonite from corals and pteropods, and calcite from coccolithophorids and foraminifera (Feely et al., 2004). As the oceans become enriched in anthropogenic CO<sub>2</sub>, the chemistry of the ocean is changing because the calcium carbonate saturation state is decreased especially in cooler mid-high latitude environments (Kleypas et al., 2006). A reduction of 20-30% of mean carbonated ions has been observed in surface seawaters (Feely et al., 2004). The dissolution of particulate organic carbon in the ocean affects the calcification rates of organisms, which are predicted to decrease by 40% until 2100 if anthropogenic CO<sub>2</sub> emissions are not reduced (Andersson et al., 2006). Biogenic calcification rates are predicted to fall below the CaCO<sub>3</sub> dissolution rate, meaning that CaCO<sub>3</sub> would be dissolving faster than it is being produced (Andersson et al., 2006). The impacts of ocean acidification may be first witnessed in coastal ecosystems which express higher variability in carbonate chemistry and are more unstable environments compared to the deep sea (Feely et al., 2004; Andersson et al., 2006; Harris et al., 2013).

Shell calcification processes in marine organisms can be affected by ocean acidification as has been documented for a number of molluscan taxa (Gaylord et al., 2011; Coleman et al., 2014; Queirós et al., 2015; Marshall et al., 2019; Doney et al., 2020). The scientific literature on the effects of ocean acidification on molluscs has expanded rapidly indicating a general trend of shell growth reduction under low pH conditions. For example, *Nucella lamellosa* in Canada inhibited its shell growth when exposed for a very short period (6 days) to a pH treatment that was 0.2-0.4 units lower than ambient (Nienhuis et al., 2010). Ries et al. (2009) indicated that shell calcification of *Littorina littorea* and *Urosalpinx cinerea* was reduced after exposure to low pH (0.1–0.2 units) for a period of 60 days. *Strombus luhuanus* suffered a significant reduction of growth even after a very moderate pH decrease (0.04 units) over a 6-month period (Shirayama and Thornton, 2005). However, shell growth of some other species such as *Nassarius festivus* in Hong Kong was not significantly affected by reduced pH (950 and 1250  $\mu$ atm for 31 days) (Zhang et al., 2016), thus indicating that sensitivity to ocean acidification is species-specific and needs to be explored in fine detail (Doney et al., 2020). Similarly, shell growth of *Nucella ostrina* was not affected when pH was reduced by 0.5 units for a period of 6 months, although its shell became 10% weaker under predation cues (Barclay et al., 2019). Temperature as a factor alone has been also proven to affect the formation of mollusc shells, such as in *Chamelea gallina* that formed lighter, thinner and more porous shells at higher temperatures resulting in reduced shell fracture load (Gizzi et al., 2016). Furthermore, the combined effect of low pH (7.8) and increased temperature (28°C) in the pearl oyster *Pinctada fucata* significantly reduced the net calcification rate, as well as the calcium and carbon shell contents (Li et al., 2016).

The gastropod shell is enlarged by deposition of minerals from the outer edge of the mantle to the aperture lips and consists of four layers, the outer periostracum that is composed of conchin and three more CaCO<sub>3</sub> layers (Ruppert and Barnes, 1996). Three different polymorphs of biogenic CaCO<sub>3</sub> structures have been found in marine shells (aragonite, calcite and vaterite) that represent complex composites of one or more mineral phases and organic molecules (Nehrke et al., 2012). Calcifiers can adjust their shell strength and properties, which depend on the thickness and packing (i.e., porosity) of calcium carbonate crystals, in order to build more durable shells under ocean acidification conditions (Leung et al., 2020). Ocean acidification might be causing a shift to a more disorganized crystallographic structure in shells, thus reducing their structural integrity and the ability of marine calcifiers to biomineralise (Fitzer et al., 2015).

Some marine calcifiers will still be able to maintain synthesis of their shells even when external seawater parameters are thermodynamically unfavorable for the formation of CaCO<sub>3</sub> because they can increase fluid pH and carbonate ion concentration at the very local site of crystal nucleation (DeCarlo et al., 2018). Shells that are composed by the less soluble form of CaCO<sub>3</sub> (low-Mg calcite) will be less affected than others (Leung et al., 2017b). According to Ries et al. (2009), species exhibiting increased skeletal or shell dissolution under acidified conditions are mainly composed of the more soluble aragonite and high-Mg calcite CaCO<sub>3</sub> polymorphs. Shell thickness of *Subnivalia undulata* was found to be more resilient to ocean acidification, which might be the result of the more robust periostracum layer that reduces the rate of shell dissolution (Coleman et al., 2014). On the contrary, the Japanese tritons *Charonia lampas* suffered increased dissolution and significant corrosive effects under acidification conditions especially in the older parts of their shell, which resulted in smoother, thinner and less dense shells (Harvey et al., 2018). *Tegula funebris* showed signs of dissolution on the exterior of their shells when exposed to 0.5 pH units lower than ambient for 6 months, which was attributed to the increased presence of crystal edges and faces on their outer fibrous calcite layer potentially increasing the surface area on which dissolution can occur (Barclay et al., 2020). Thicker and architecturally more diverse shells are a fitness advantage for molluscs as an adaptation to predators (Fisher et al., 2009). Ocean acidification may not only lead to increased fragility of shells but may also elevate energetic costs for shell formation or repairing (Leung et al., 2020). The capacity of molluscs to maintain their shell calcification mechanisms under altered environmental conditions will regulate their successful adaptation and persistence in the future. Shell growth measured traditionally as shell length may continue to develop normally, even under acidified and adverse climatic conditions; however, the newly produced shells might be thinner and more fragile (Byrne and Fitzer, 2019).

In the present study, the individual and combined effects of low pH and high temperature were tested on two gastropod species, *Nassarius nitidus* and *Columbella rustica* (superfamily Buccinoidea). *N. nitidus* is a scavenger able to withstand a great range of salinity and temperature ranges commonly found to low sublittoral and intertidal areas (up to 15 m depth)

(Eriksson and Tallmark, 1974). *C. rustica* is a herbivore (Taylor, 1987) and a scavenger or occasional carnivore (Starmühlner, 1969) living between rocks and in silt patches of the midlittoral zone (Delamotte and Vardala-Theodorou, 2007). Both species are abundant in the Mediterranean and are well adjusted to temperature and pH alterations since they inhabit coastal systems such as rock pools and lagoons where such fluctuations of environmental conditions are common (Wahl et al., 2016). Both species have shells consisting of the more soluble aragonite material (Bouillon, 1958; Cespuglio et al., 1999; Foster and Cravo, 2003), while in other gastropod species a more resistant mixture of low magnesium calcite and aragonite can be found (Ries et al., 2009). The morphological properties of the shell of the abovementioned two species, and more specifically their shell density, thickness and closed porosity, were examined using an advanced 3D imaging and analytical technique (3D micro-computed tomography). This method offers an additional insight in the internal shell micro-structure of the selected gastropods since it allows measurements of specific architectural parameters of the full intact shell. The selected treatments were based on the high emissions RCP 8.5 scenario of the Intergovernmental Panel on Climate Change models for the eastern Mediterranean until the year 2100 (IPCC, 2014), which is commonly referred to as the “business as usual” scenario, suggesting that this is a likely outcome if the society does not make any concerted efforts to cut greenhouse gas emissions.

## MATERIALS AND METHODS

### Specimen Selection and Experimental Setup

*Nassarius nitidus* specimens ( $n = 48$ ; size range 17.7–20.8 mm; mean shell length  $19.5 \pm 0.8$  mm) were collected from subtidal lagoons (1 m depth) in Amvrakikos Bay (Western Greece) ( $39^{\circ}3'41''\text{N}$ ,  $20^{\circ}48'14.3''\text{E}$ ) and *Columbella rustica* ( $n = 36$ ; size range 10.1–12.3 mm; mean shell length  $11.1 \pm 0.7$  mm) were collected from the coast of Gournes (Heraklion, North Crete) ( $35^{\circ}20'06.0''\text{N}$ ,  $25^{\circ}16'43.9''\text{E}$ ). Acclimatization of gastropods lasted about one month (rate: 0.05 units/10 days for pH;  $0.7^{\circ}\text{C}/10$  days for temperature). Organisms were maintained following standard aquarist practices and were fed *ad libitum*. The mean ambient temperature in the natural environment was  $20^{\circ}\text{C}$  and in the warm treatments it was  $23^{\circ}\text{C}$  (future RCP 8.5 scenario prediction - increase of  $3^{\circ}\text{C}$ ). The ambient pH was 8 and the low pH treatment was 7.7 (future RCP 8.5 scenario prediction - decrease of 0.3 units). The gastropods were equally divided per experimental treatment (i.e., 12 *N. nitidus* and 9 *C. rustica* per treatment), placed in individual tanks (2–4 l) and maintained under the following four experimental treatments for a total period of three months (88 days): a) one control with ambient temperature ( $20^{\circ}\text{C}$ ) and pH (pH = 8) (code tank 8A), b) one with ambient temperature ( $20^{\circ}\text{C}$ ) and low pH (pH = 7.7) (code tank 7A), c) one with warmer temperature ( $23^{\circ}\text{C}$ ) and ambient pH (pH = 8) (code tank 8W) and d) one with warmer temperature ( $23^{\circ}\text{C}$ ) and low pH conditions (pH = 7.7) (code tank 7W).

A semi-closed experimental system was used to ensure controlled experimental conditions (for details see Chatzinikolaou et al., 2017). Submerged aquarium heaters (RESUN) were used to rise temperature to the desired level in the warm treatments. A bubbling  $\text{CO}_2$  system attached to the  $\text{CO}_2$  bottles through a manometer (Gloor model 5100/10) and connected to a pH controller system (Tunze 7070/2) was used to adjust the low pH treatments. The pH electrodes were calibrated twice every month with 5.00, 7.00 and 10.00 WTW NBS buffers. Temperature and pH (on the National Bureau of Standards scale - $\text{pH}_{\text{NBS}}$ ) were additionally measured daily (3420 WTW multi-meter), while salinity (salinometer) and oxygen (OxyGuard) were checked every two days. A submerged pump (Boyo WM-15) with additional airstones was used to ensure sufficient water circulation. In addition, 50% of the water in the experimental tanks was renewed twice a week thus maintaining a high water quality within the system ( $\text{NO}_2 < 0.1$  mg/l,  $\text{NO}_3 < 0.5$  mg/l,  $\text{NH}_3/\text{NH}_4 < 0.2$  mg/l). Nitrogenous waste products were also assessed twice a week by using photometric test kits (Tetra kit). Total alkalinity (TA) was measured every two weeks according to the Standard Operating Procedure (SOP 3b) described in Dickson et al. (2007) using an open-cell titration (Metrohm Dosimat 765; 0.1 mol/kg in HCl). Measured parameters (pH and TA) were used to calculate the additional parameters of the seawater carbonate system (**Supplementary Material - Table I**) using CO2SYS program with the dissociation constants of Mehrbach et al. (1973) as refitted by Dickson and Millero (1987).

Three individuals of each species were randomly collected from each treatment at the end of the experiment (3 months). Specimens were anesthetized using a rising concentration of  $\text{MgCl}_2$  starting at 1.5% and gradually reaching 3.5% according to the European Directive 2010/63 EU on the protection of animals used for scientific purposes. The samples were stored at  $-20^{\circ}\text{C}$  until scanning was performed.

### Scanning and Reconstruction of Images

All scans were performed with a SkyScan 1172 micro-tomograph (Bruker, Kontich, Belgium) at the Hellenic Center for Marine Research (HCMR). The scanner uses a tungsten source and is equipped with an 11 PM CCD camera ( $4,000 \times 2,672$  pixels), which can reach a maximal resolution of  $<0.8 \mu\text{m}/\text{pixel}$ . Specimens were scanned at a voltage of 70 kV and a flux of  $142 \mu\text{A}$  with an aluminum filter of 0.5 mm and images were acquired at a pixel size of  $6.51 \mu\text{m}$  with a camera binning of  $1 \times 1$ . Exposure time was 6,455 msec for *N. nitidus* and 7,005 msec for *C. rustica* specimens. Scans were performed for a half rotation of  $180^{\circ}$  to minimize scanning duration, since initial tests had shown there was no significant loss of information or increase of artifacts compared to a full rotation. All scans were performed over a short period of time without recalibrating the instrument's settings and using the exact same scanning parameters in order to ensure full comparability of the results.

Projection images were reconstructed into cross sections using SkyScan's NRecon software (Bruker, Kontich, Belgium) which employs a modified Feldkamp's back-projection algorithm.

The scans of the same species were reconstructed using the same range of attenuation coefficients (*N. nitidus*: 0.04 - 0.16, *C. rustica*: 0.00 - 0.21) in order to obtain comparable results. The reconstructed images were stored as 8-bit PNG images due to storage limitations, since initial comparisons had shown no significant differences ( $p > 0.05$ ) in the analyses results in comparison to 16-bit TIFF images.

## Image Analysis

Cross section images were loaded into the software CT Analyzer v.1.14.4.1 (CTAn, Bruker, Kontich, Belgium) and the mean gray scale values of the total shell were calculated using the binary threshold module as a proxy for relative shell density. For the present analyses, no absolute density values (e.g., Hounsfield units) were required, but only comparability between the scans (relative densities). In the present study, density refers to micro-density (i.e., density of the shell material including  $\text{CaCO}_3$  and intraskeletal organic matrix) and not to bulk density which includes porosity. The range of the gray scale histogram was the same for specimens of the same species (*N. nitidus*: 1-255, *C. rustica* 40-255).

The 3D analysis was performed in each micro-CT scan using the custom processing plug-in of CTAn software, in order to calculate the closed porosity of the shell, which is the total volume of enclosed pores of each specimen, defined as a % percentage of the total shell volume. Porosity can be connected to the outer surface of the shell (open porosity) or not (closed porosity). A 3D model of the closed pores for each gastropod species was generated by the creation of a surface mesh of the closed pores using CTAn software, which was then visualized using the CTVol software (Bruker, Kontich, Belgium).

The structure thickness of each specimen was calculated using 3D analysis in CTAn software through the application of the “sphere-fitting” measurement (i.e., estimation of the mean of the diameters of the largest spheres which can be fitted in each point of the selected shell structure) (Hildebrand and Rügsegger, 1997). Finally, a color-coded dataset was created for structure thickness in CTAn software in order to visualize the structure thickness distribution throughout each specimen. The 3D model of the structure thickness distribution was visualized through the CTVox software (Bruker, Kontich, Belgium).

## Statistical Analyses

Statistical analyses were conducted using the software Minitab (version 13.2). Prior to analyses, all data were checked for normality distribution (Anderson-Darling test; normal for  $p > 0.05$ ) and homogeneity of variances (Bartlett's test; equal variances for  $p > 0.05$ ). Since all data were normal and had equal variances, one-way ANOVA tests were used to test differences between treatments in density, porosity and structure thickness for both species. When necessary, *post hoc* analysis (Tukey's tests) was performed to determine the significance of the factors interaction. Significant differences were considered at a threshold of  $\alpha = 0.05$ . Confidence intervals for the Tukey's tests are considered significant when they are not including the zero value.

## RESULTS

Mean density, structure thickness and % of closed porosity for the four treatments are presented in **Figure 1** for *Nassarius nitidus* and in **Figure 2** for *Columbella rustica*. Results for statistical comparisons are presented in **Tables 1, 2**, while Tukey's *post hoc* tests are presented in **Supplementary Material - Table II**. None of the comparisons performed for the morphological parameters of the *N. nitidus* full shell indicated statistically significant differences between the four treatments (**Table 1**,  $p > 0.05$ ). The increased variability observed between individuals and the relatively low number of specimens due to the logistical constraints of performing a micro-CT analysis could possibly be the reason for this limited statistical significance; however, the observed trends can still offer a useful insight in shell architecture of *N. nitidus* and therefore the respective data presented in **Figure 1** are being further described. *Nassarius nitidus* had a lower mean shell density and a lower mean structure thickness in the 7A treatment (low pH, ambient temperature) in comparison to all other treatments; however these differences were not statistically significant ( $p > 0.05$ ). The 8A control treatment (ambient pH and temperature) had the highest mean density and thickness (**Figures 1A,B** and **Table 1**). The combination of low pH and warm temperature (7W) was not detrimental for *N. nitidus* since the respective values were more similar to the control (8A). Mean porosity of the *N. nitidus* shell appears to be increased in all treatments in comparison to the control (**Figure 1C**), although again here the increased variability between individuals eliminated the statistical significance of these differences. The 3D models used for the visualization of *N. nitidus* closed porosity for all treatments are presented in **Figure 3**. Increased porosity in both low pH treatments (7A and 7W, **Figures 3A,C**, respectively) is seen around the shell lip, while in both warm treatments porosity is increased closer to the shell apex (7W and 8W, **Figures 3C,D**, respectively).

*Columbella rustica* indicated lower variability between individuals in comparison to *N. nitidus* (**Tables 1, 2**). The shell density of *C. rustica* in acidified and warmer conditions (7W) was significantly lower in comparison to all other treatments ( $p < 0.001$ , see **Table II** in **Supplementary Material** for all *post hoc* comparisons). On the contrary, when the temperature was increased but the pH remained at ambient values (8W), shell density was significantly higher than all other treatments ( $p < 0.001$ ), including the control (**Figure 2A**). The exact same pattern was observed for structure thickness of the total shell in *C. rustica* (**Figure 2B**). Shells under acidified and warmer conditions (7W) were significantly thinner, while shells in warmer but ambient pH conditions (8W) were significantly thicker ( $p < 0.001$ ). In addition, the % of closed porosity was significantly higher (more than double) in the acidified and warmer conditions (7W) in comparison to all other treatments (**Figure 2C** and **Table 2**,  $p = 0.015$ ). The 3D models used for the visualization of *C. rustica* closed porosity for all treatments are presented in **Figure 4**, where increased porosity can be seen in the acidified and warm treatment (7W, **Figure 4C**).

The distribution of structure thickness as % percentage of the shell volume for all the four treatments and for both species is

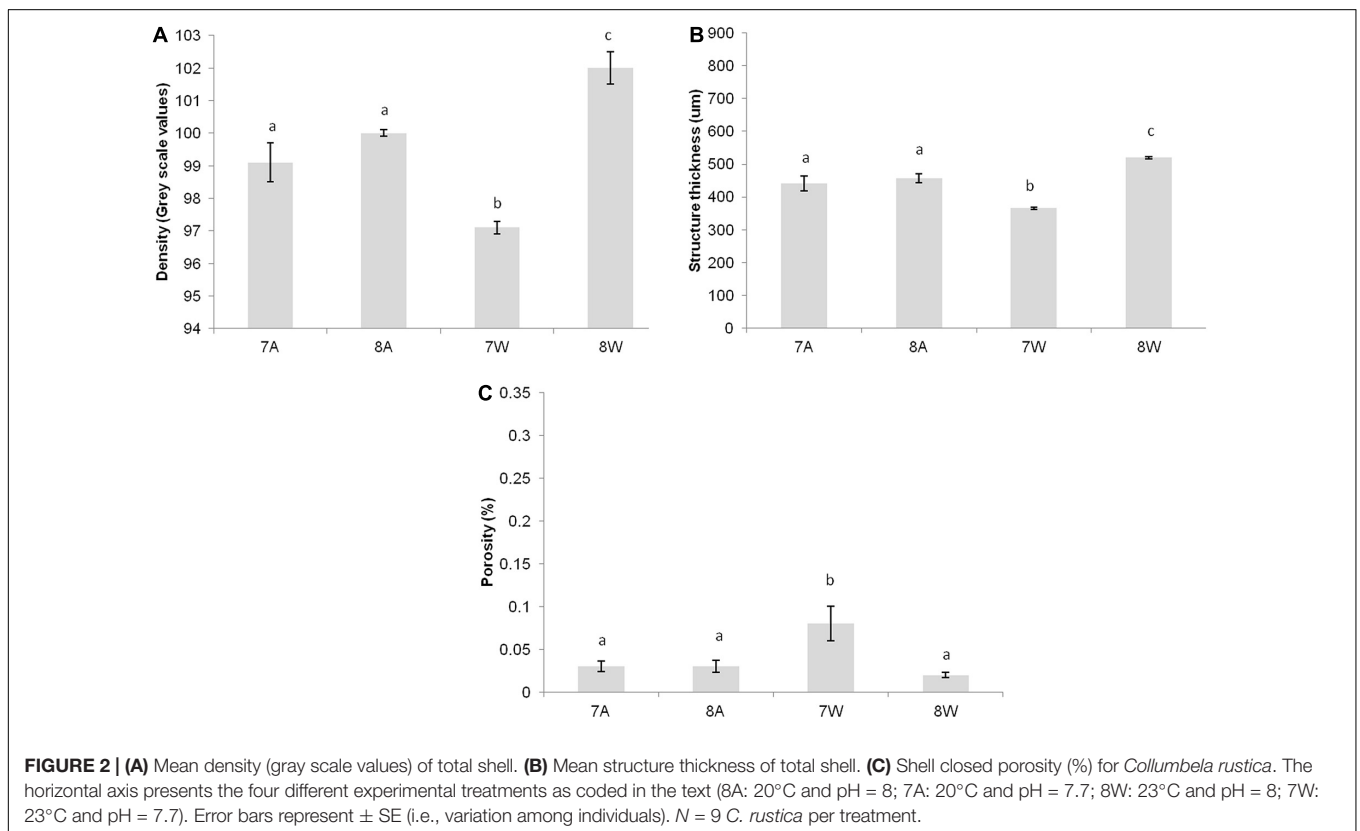
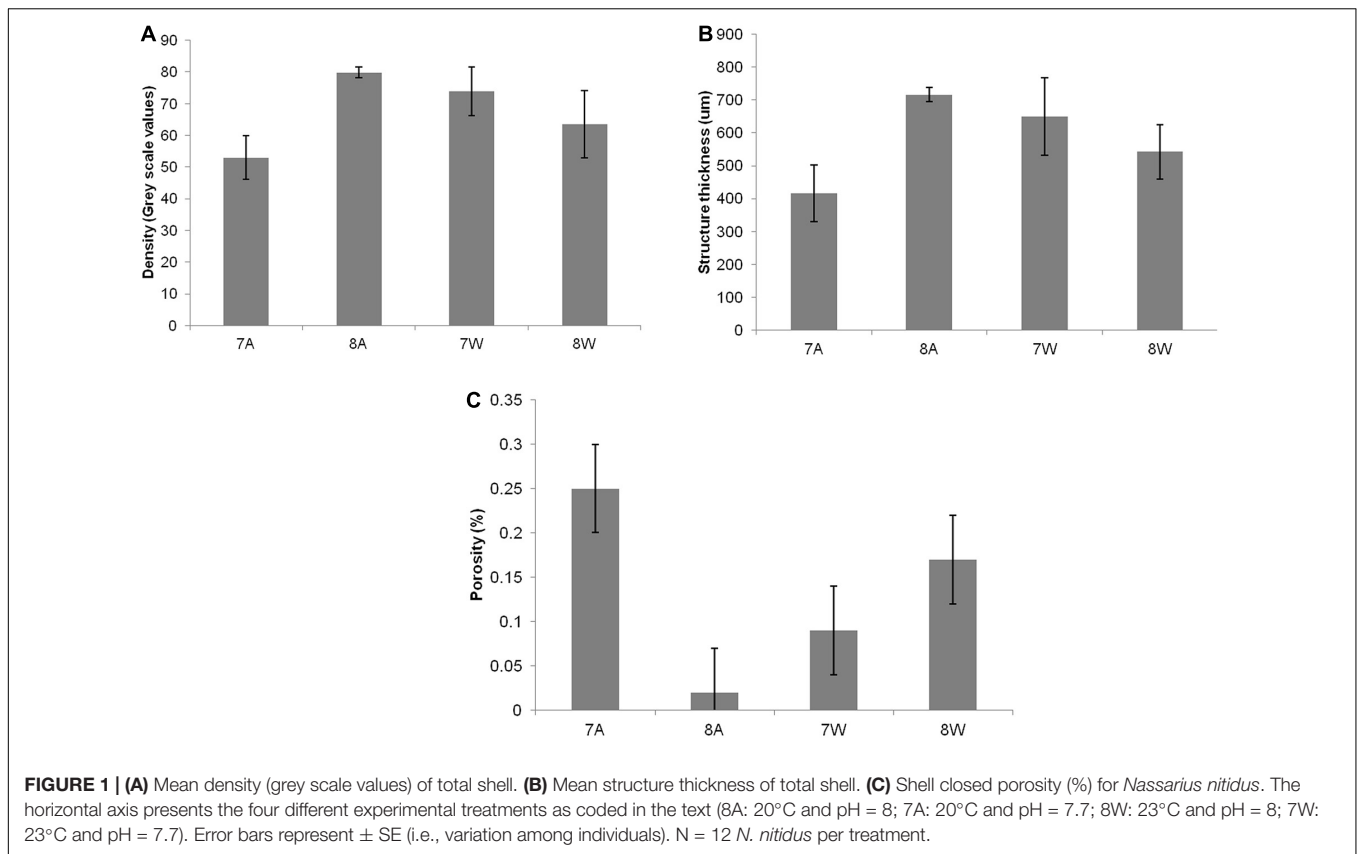


**TABLE 1** | Mean density (gray scale values) of the total shell, structure thickness (um) and porosity% ( $\pm$  SE) for *Nassarius nitidus* in the four experimental treatments A (7A), B (8A), C (7W), and D (8W) as coded in the text (8A: 20°C and pH = 8; 7A: 20°C and pH = 7.7; 8W: 23°C and pH = 8; 7W: 23°C and pH = 7.7).

<i>Nassarius nitidus</i>			
Treatment	Density (gray scale)	Structure thickness (um)	Porosity%
7A	52.9 ( $\pm$ 6.9)	416.4 ( $\pm$ 86.8)	0.25 ( $\pm$ 0.10)
8A	79.8 ( $\pm$ 1.7)	716.1 ( $\pm$ 21.8)	0.02 ( $\pm$ 0.01)
7W	73.9 ( $\pm$ 7.6)	650.2 ( $\pm$ 118)	0.09 ( $\pm$ 0.07)
8W	63.4 ( $\pm$ 10.6)	542.1 ( $\pm$ 81.9)	0.17 ( $\pm$ 0.07)
ANOVA	F = 2.56, p = 0.128	F = 2.40, p = 0.143	F = 1.87, p = 0.212

Results of statistical tests (ANOVA or Kruskal Wallis) and significance (\*) are indicated. N = 12 *N. nitidus* per treatment.

**TABLE 2** | Mean density (gray scale values) of the total shell, structure thickness (um) and porosity% ( $\pm$  SE) for *Columbella rustica* in the four experimental treatments A (7A), B (8A), C (7W), and D (8W) as coded in the text (8A: 20°C and pH = 8; 7A: 20°C and pH = 7.7; 8W: 23°C and pH = 8; 7W: 23°C and pH = 7.7).

<i>Columbella rustica</i>			
Treatment	Density (gray scale)	Structure thickness (um)	Porosity%
7A	99.1 ( $\pm$ 0.6)	440.8 ( $\pm$ 22.2)	0.03 ( $\pm$ 0.006)
8A	100.0 ( $\pm$ 0.1)	457.1 ( $\pm$ 13.9)	0.03 ( $\pm$ 0.007)
7W	97.1 ( $\pm$ 0.2)	365.3 ( $\pm$ 3.8)	0.08 ( $\pm$ 0.020)
8W	102.0 ( $\pm$ 0.5)	519.7 ( $\pm$ 3.2)	0.02 ( $\pm$ 0.003)
ANOVA	F = 24.97, p < 0.001*	F = 22.66, p < 0.001*	F = 6.58, p = 0.015*

Results of statistical tests (ANOVA or Kruskal-Wallis) and significance (\*) are indicated. N = 9 *C. rustica* per treatment.

presented in **Figures 5A,B**. The CTAn 3D analysis indicated a maximum total number of 132 classes with a range of 13 um each for *N. nitidus*, which were grouped as 17 classes with a range of about 100 um for each class to facilitate graphical presentation. Similarly, a maximum total number of 92 classes with a range of 13 um each was estimated for *C. rustica*, which were grouped as 12 classes with a range of about 100 um for each class.

The thickness of the *N. nitidus* shell under normal conditions (8A) ranges up to a maximum of 1608.7 um and the highest percentage of values (peak of the distribution) is found within the range of 605.7 – 709.9 um (**Figure 5A**). Gastropods under acidified conditions (7A) present a shift of their thickness distribution toward lower values and in this case the highest percentage is found within the range of 110.7 – 501.5 um (74.8%). The shell thickness distribution of *N. nitidus* which have been maintained under a combination of increased temperature and low pH (7W) is more similar to the control one (also peaks at 605.7 – 709.9 um), but again in this case a higher percentage is found within the region of lower (i.e., less dense) values (< 306.1 um). Gastropods under normal pH but warmer temperature (8W) have a peak distribution at 501.5-605.7 um and again present higher percentages at lower thickness values

(< 397.3 um) in comparison to the control. A statistical comparison (ANOVA) of each thickness class separately between the four treatments confirms the above suggestions and indicates significant differences between the classes 201.9 – < 306.1 ( $F = 4.65$ ,  $p = 0.036$ ), 306.1 – < 397.3 ( $F = 5.53$ ,  $p = 0.024$ ), 397.3 – < 501.5 ( $F = 4.66$ ,  $p = 0.036$ ), 605.7 – < 709.9 ( $F = 4.27$ ,  $p = 0.045$ ) and 709.9 – < 801.1 ( $F = 3.77$ ,  $p = 0.050$ ).

The shell thickness of *C. rustica* under normal conditions (8A) ranges up to a maximum of 1009.5 um and the peak of the distribution is found within the range of 397.3-501.5 um (**Figure 5B**). Gastropods under acidified and ambient temperature conditions (7A) present a similar distribution pattern with 8A with the same maximum thickness value and the same peak for the highest percentage. When the temperature is higher, the distribution peak remains within the same range as the control, but low pH treatment (7W) results in more values toward the thinner ranges (78.4% of the shell volume with thickness <501.5 um), while normal pH (8W) results in more values toward the thicker ranges (73% of the shell volume with thickness >397.3 um). Also *C. rustica* under higher temperature with normal pH (8W) develop shells that reach greater maximum thickness values (up to 1204.9 um) than all the other treatments. A statistical comparison (ANOVA) of each thickness class separately between the four treatments confirms the above suggestions and indicates significant differences between the classes <110.7 um ( $F = 10.29$ ,  $p = 0.006$ ), 110.7-201.9 um ( $F = 22.33$ ,  $p = 0.001$ ), 201.9 – <306.1 ( $F = 7.65$ ,  $p = 0.013$ ), 605.7 – < 709.9 ( $F = 8.13$ ,  $p = 0.011$ ) and 709.9 – < 801.1 ( $F = 5.11$ ,  $p = 0.035$ ), as well as for classes >1009.5 ( $F = 12.58$ ,  $p = 0.003$ ) where only samples of 8W were found.

Although the statistical analysis of the full shell thickness did not indicate significant differences between the experimental treatments in *N. nitidus* ( $p > 0.05$ , **Table 1**) due to the increased variability between samples, the 3D color coded images constructed by the micro-CT analysis (CTVox) (**Figure 6**) and the subsequent comparisons between separate thickness classes (**Figure 5A**) revealed a clear degree of differentiation. Gastropods in low pH and ambient temperature (7A) had a very thin shell throughout its total structure (**Figure 6A**), obviously different from all other treatments. The control treatment shell (8A) is the one that visually presented the thickest areas (**Figure 6B**). The sample from the combined low pH - high temperature (7W) treatment had also a similar thickness pattern with the control (**Figure 6C**) with thicker areas located along the shell ribs and lip. The warm but ambient pH treatment (**Figures 6D, 8W**) was not as severely thin as the 7A was, but revealed some distinct areas close to the siphon canal and the shell lip which appeared thinner in comparison to the control.

The 3D color coded images for *C. rustica* thickness (**Figure 7**) and the subsequent comparisons between separate thickness classes (**Figure 5B**) indicated a clear visual pattern of the impact of low pH and increased temperature in the shell structure of this species. Specimens treated under low pH and increased temperature (7W, **Figure 7C**) appeared thinner especially around the opening of the shell, which was also obvious for specimens treated under low pH and ambient temperature (7A, **Figure 7A**). The control shell (8A, **Figure 7B**) is clearly thicker and the

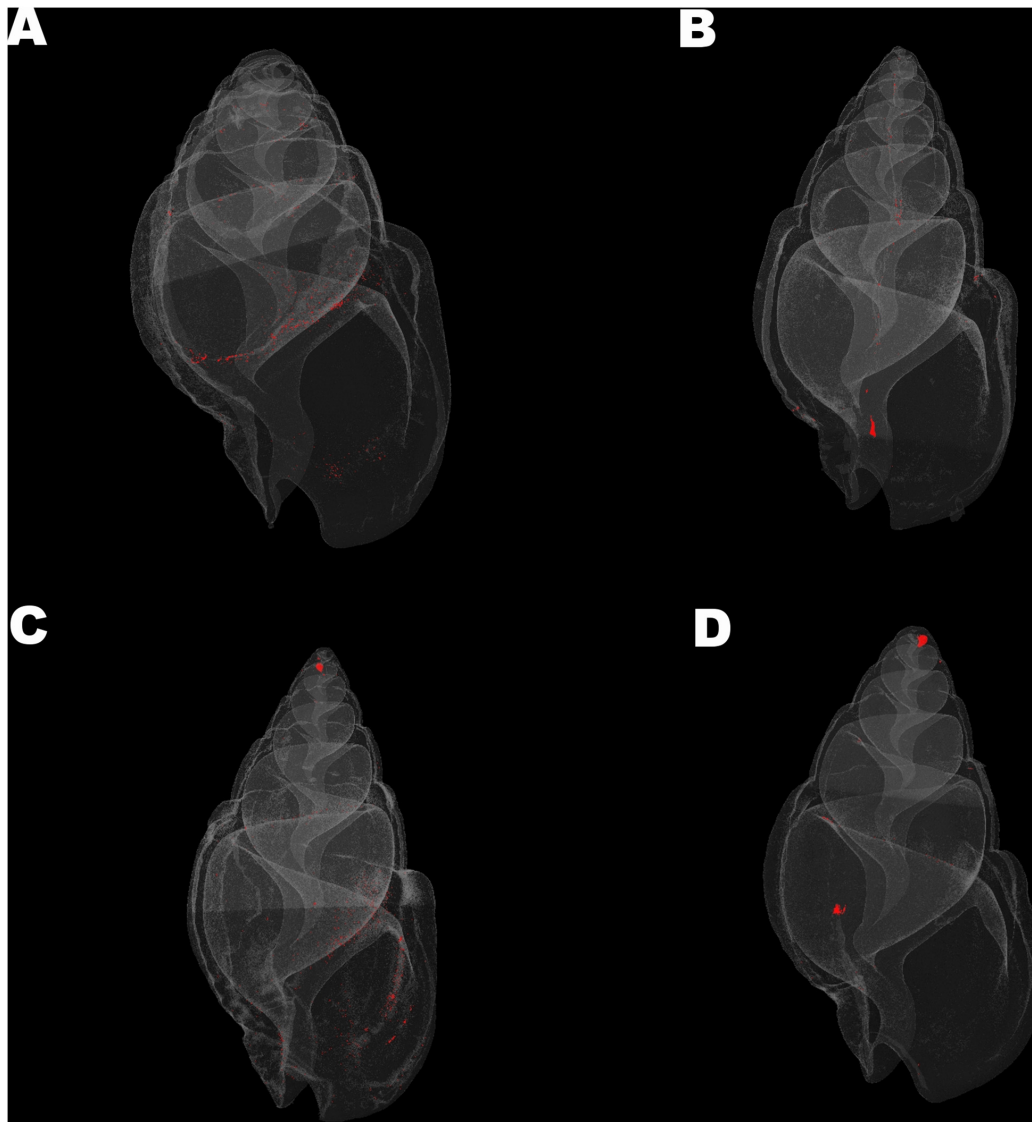


**FIGURE 3** | Visualization of shell closed porosity for *Nassarius nitidus* in the four experimental treatments **(A)** (7A), **(B)** (8A), **(C)** (7W), and **(D)** (8W) as coded in the text (8A: 20°C and pH = 8; 7A: 20°C and pH = 7.7; 8W: 23°C and pH = 8; 7W: 23°C and pH = 7.7).

shell surface appears also smoother in comparison to shells of acidic conditions. The gastropods shells maintained under higher temperature but normal pH (8W, **Figure 7D**) were also thickened around the opening and lip, as was also confirmed by the average shell values of the 3D analysis (**Table 2**,  $p < 0.001$ , Tukey's *post hoc* tests in Table II, **Supplementary Material**).

## DISCUSSION

The shell degradation of gastropods as a result of ocean acidification (low pH) has been documented in previous studies for several species (Bibby et al., 2007; Gazeau et al., 2013; Melatunan et al., 2013; Queirós et al., 2015; Chatzinikolaou et al., 2017; Harvey et al., 2018; Barclay et al., 2020). The capacity of

marine organisms to construct calcium carbonate ( $\text{CaCO}_3$ ) shells and skeletons can be impaired by reduced pH (Doney et al., 2009). It is evident that such impacts are very much species specific and for some species the effects are more detrimental than others (Byrne and Fitzer, 2019; Barclay et al., 2020). Building and maintaining marine biomaterials under ocean acidification depends on the balance between calcification and dissolution, while ocean warming has the potential to ameliorate or highlight some of the negative effects on shell strength and elasticity (e.g., weaker shells with less dense biominerals and increased porosity) (Byrne and Fitzer, 2019). Therefore, it is interesting to compare the shell morphological characters of different species which are living in different micro-habitats or are characterized by different modes of life, in order to define what might be the factors of increased susceptibility for some specific species

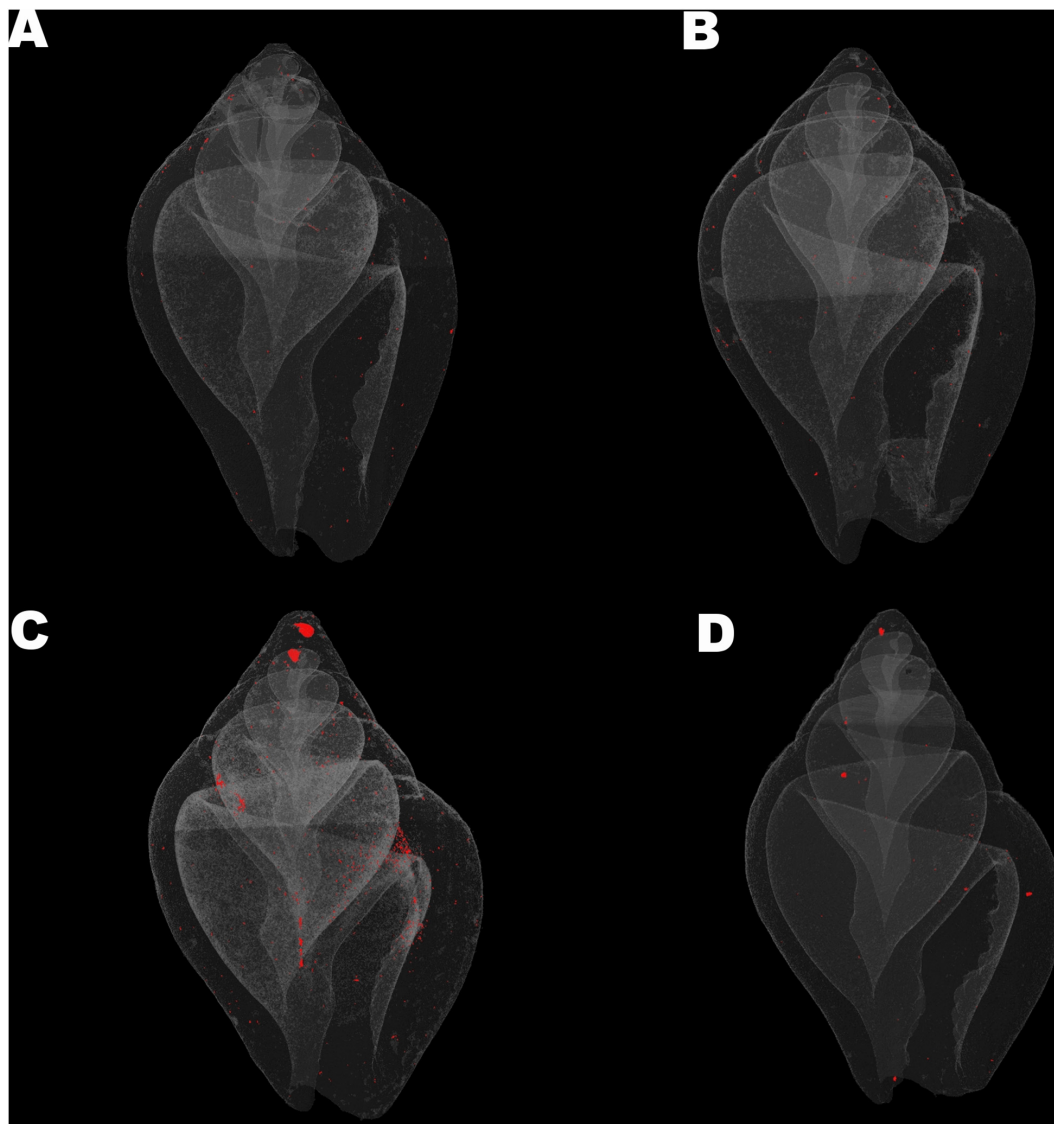


**FIGURE 4** | Visualization of shell closed porosity for *Collumbela rustica* in the four experimental treatments **(A)** (7A), **(B)** (8A), **(C)** (7W), and **(D)** (8W) as coded in the text (8A: 20°C and pH = 8; 7A: 20°C and pH = 7.7; 8W: 23°C and pH = 8; 7W: 23°C and pH = 7.7).

in comparison to others. Different species are characterized by different vulnerability and tolerance responses regarding ocean acidification and warming, and this variability may affect their ecological interactions and the respective marine habitat biodiversity (Chatzinikolaou et al., 2017). The effects of ocean acidification on the growth and shell production by juvenile and adult shelled molluscs are variable among species and even within the same species, precluding the drawing of a general picture (Gazeau et al., 2013). Conventional metrics previously used to quantify shell growth need to be enriched with methods for evaluating changes to biomineral structure and mechanical integrity caused by ocean acidification (Byrne and Fitzer, 2019).

The authors of the present study have previously investigated the effects of acidic conditions on the density of specific shell regions of *Nassarius nitidus* and they have reported a reduction of

38.1% in the shell lip, 51.4% in the lip distal (newest regions) and 47.7% in the apex (oldest region) (Chatzinikolaou et al., 2017). In the present study, a more thorough examination for the same species was performed during which the full shell was examined instead of isolated shell regions. In addition, while the previous study investigated only differences in shell density, the present study also investigated additional morphological characters of the shell, such as enclosed porosity and thickness. Although the results of the present study did not indicate statistically significant differences between treatments for *N. nitidus*, they can still be considered as a valuable informative insight into the architectural shell properties of this species using an innovative 3D imaging analysis technique. As observed in the present study, low pH affected (although not significantly) the average density and structure thickness of the total shell in *N. nitidus* when

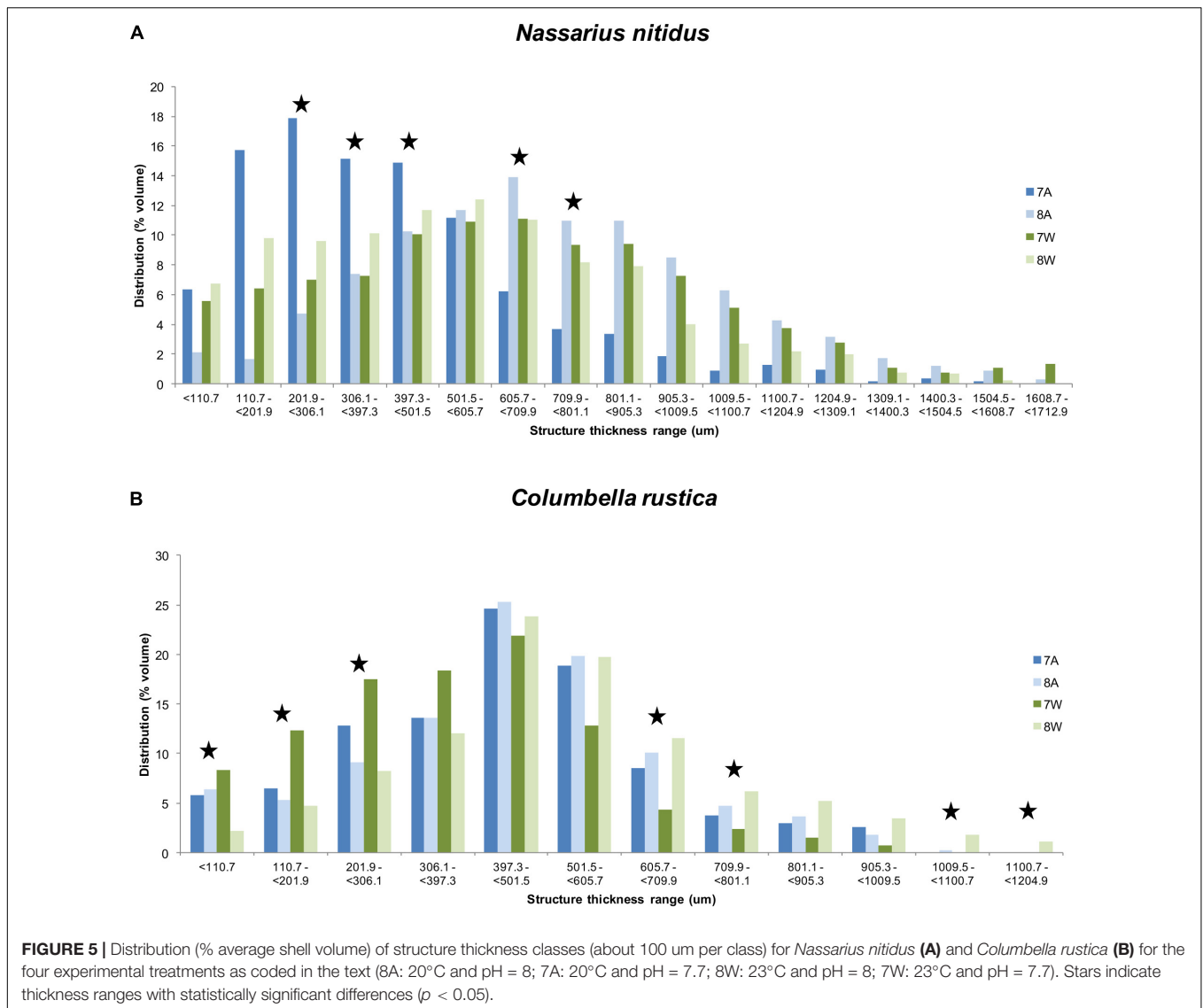


**FIGURE 5 |** Distribution (% average shell volume) of structure thickness classes (about 100  $\mu\text{m}$  per class) for *Nassarius nitidus* (A) and *Columbella rustica* (B) for the four experimental treatments as coded in the text (8A: 20°C and pH = 8; 7A: 20°C and pH = 7.7; 8W: 23°C and pH = 8; 7W: 23°C and pH = 7.7). Stars indicate thickness ranges with statistically significant differences ( $p < 0.05$ ).

temperature was at ambient levels. Furthermore, when thickness classes were separately examined, *N. nitidus* shell had a significant shift toward thinner values at lower pH, and this was especially evident in ambient temperatures. The significant differences revealed when thickness classes were examined separately maybe the result of increased variability observed between individuals. The 3D visual analysis of structure thickness also confirmed that the whole shell has suffered extensive damages and erosion. However, when the temperature was increased *N. nitidus* somehow compensated for the shell loss caused by the acidic conditions (7W), presumably by accelerating shell production processes. The effect of elevated seawater temperature has been previously correlated with an increase in the growth of this genus, such as in *N. reticulatus* (Barroso et al., 2005; Chatzinikolaou and Richardson, 2008) and *N. festivus* (Morton and Chan, 2004). Also *Columbella rustica* in the present study formed significantly denser and thicker shells, especially around the lip, when the temperature was higher (8W) thus indicating an acceleration

of shell growth and calcification processes which has been commonly observed in several gastropod species, even seasonally under ambient conditions (Morton and Chan, 2004; Barroso et al., 2005; Chatzinikolaou and Richardson, 2008). The amount of energy available for growth is determined by the ingestion and the respiration rate of an organism, which are indeed functions related to temperature (Hughes, 1986).

The combined impact of low pH and increased temperature was clearly disadvantageous for *C. rustica*, indicating that a negative future scenario of climate change as suggested by IPCC could be detrimental. The average shell density and thickness of *C. rustica* in acidified and warmer conditions were significantly reduced in comparison to all other treatments, while % porosity (i.e., the number of enclosed pores in reference to the total shell volume) was significantly higher. The number of pores in *C. rustica* shell under such stressful conditions was more than double in comparison to gastropods maintained under ambient conditions. Porosity is an important indicator of mechanical

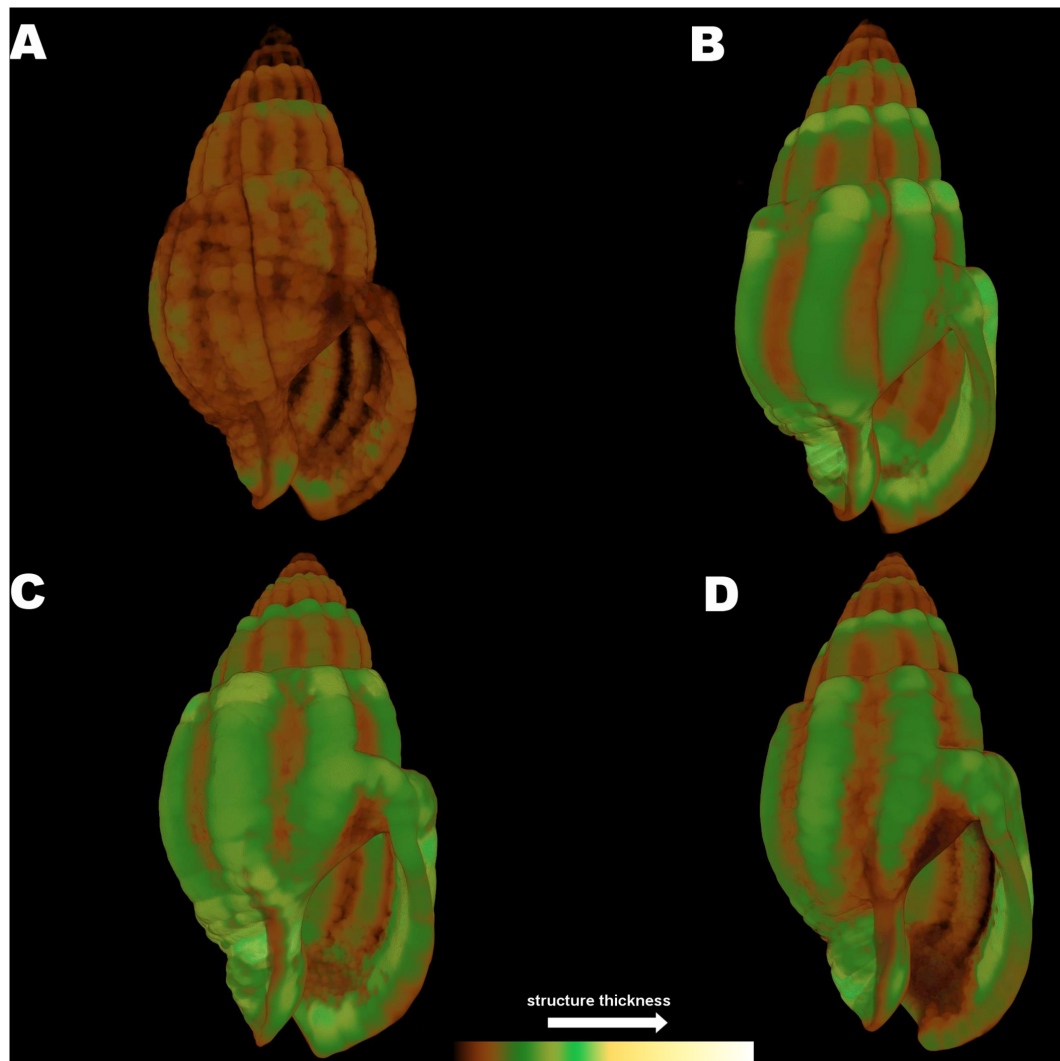


**FIGURE 6** | Color coded visualization of shell structure thickness for *Nassarius reticulatus* in the four experimental treatments **(A)** (7A), **(B)** (8A), **(C)** (7W), and **(D)** (8W) as coded in the text (8A: 20°C and pH = 8; 7A: 20°C and pH = 7.7; 8W: 23°C and pH = 8; 7W: 23°C and pH = 7.7). The bar on the bottom of the image indicates thickness scaling (cooler colors indicate thicker structures, warmer colors indicate thinner structures).

strength, where shells with a greater number of pores are more fragile (Leung et al., 2020). Shell pores usually penetrate all shell layers except the outermost organic layer (periostracum) and their interior is filled with organic compounds which are used for the periostracum repair (Reindl and Haszprunar, 1994). The increased% of porosity observed in *C. rustica* may be the result of an accelerated shell repair process, since the contents of the enclosed pores are important for shell secretion (Reindl and Haszprunar, 1994). Increased porosity has been also associated with a lower organic matter content of the shell, indicating less plasticity, reduced calcium carbonate nucleation and minimized crystal growth (Leung et al., 2020). Some calcifiers might adjust the packing of carbonate crystals (e.g., porosity) under ocean acidification in order to build more durable shells that will be able to absorb physical stress effectively, however this requires a costly energy budget (Leung et al., 2020).

*C. rustica* shells under acidic conditions in the present study were thinner especially around the shell lip and the apex. A previous study also indicated that the maximum reduction (8%) estimated in the shell density of this species was in the apex, which is the oldest shell part and might often be eroded (Chatzinikolaou et al., 2017). Similarly in *Nucella lapillus* low pH caused apex dissolution and a 20–30% reduction in shell lip density (Queirós et al., 2015). *Mytilus edulis* shells grown under ocean acidification conditions displayed significant reductions in shell aragonite thickness, shell thickness index and changes to shell shape, making them more vulnerable to fracture (Fitzer et al., 2015). *Mytilus californianus* larvae had thinner and weaker shells than individuals raised under present-day pH conditions indicating an aggravated vulnerability of new settlers to crushing and drilling attacks by predators (Gaylord et al., 2011). Similarly, treatment of the brachiopod *Liothyrella*

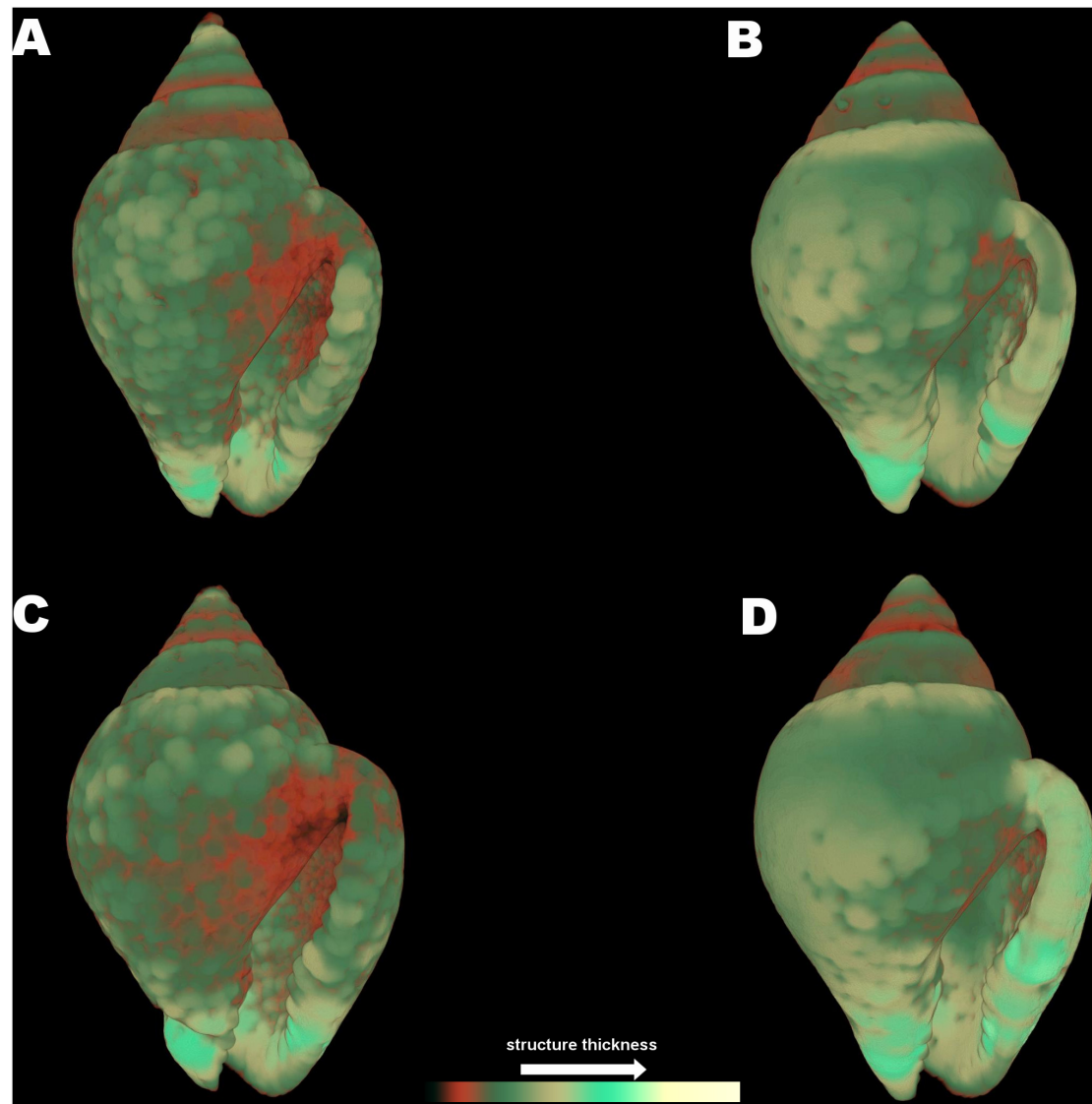


**FIGURE 7** | Color coded visualization of shell structure thickness for *Columbella rustica* in the four experimental treatments **(A)** (7A), **(B)** (8A), **(C)** (7W), and **(D)** (8W) as coded in the text (8A: 20°C and pH = 8; 7A: 20°C and pH = 7.7; 8W: 23°C and pH = 8; 7W: 23°C and pH = 7.7). The bar on the bottom of the image indicates thickness scaling (cooler colors indicate thicker structures, warmer colors indicate thinner structures).

*uva* under decreased pH resulted in substantial shell dissolution after 7 months and decreased outer primary layer thickness, while increasing temperature alone did not affect shell thickness (Cross et al., 2019). The monomineralic aragonite-producing gastropods were not able to alter the carbonate polymorph in their shells in order to produce calcite under low pH conditions and minimize shell dissolution (Leung et al., 2017a). However, the effect of ocean acidification in shell thickness is also species specific and there are indications that some species are enhancing their shell production to compete shell dissolution under unfavorable conditions. Specimens of the limpet *Patella caerulea* that were collected from a low pH CO<sub>2</sub> vent site, displayed increased thickness and a twofold increase in aragonite area fraction indicating an enhanced shell production under

acidified conditions thus managing to counteract dissolution (Langer et al., 2014). Shell thickening in the limpet *P. caerulea* was enhanced at the apex area and reduced along the flank area, also indicating region specific shell production (Langer et al., 2014).

Shell porosity is a shell architectural and morphological character that has not been yet thoroughly studied since it is not possible to estimate these values without using a non-destructive method such as the micro-CT tomography. Similarly, the estimation of shell thickness as an average value for the total shell, as well as the identification of the % percentages per thickness class is also a unique feature of this study estimated using this innovative imaging technique. The micro-computed tomography (micro-CT) allows the creation of interactive, quantitative, three-dimensional X-ray images at submicron resolution which can

be used to measure morphological characters of the calcified shell without interfering with its integrity. Previous studies have determined thickness of the gastropod shell by measuring only selected points on photographs of cross sections (Coleman et al., 2014), while the present method allows for the estimation of the average value of thickness of the full intact shell and of the% distribution of these values in different size classes, thus offering a more representative depiction of the shell structure. Even if shell growth is not directly affected by acidification conditions this does not ensure that shell functionality and efficiency also remains unaltered. For example, *Nucella ostrina* is able to maintain calcification and shell growth under acidified conditions, but the loss of carbonate material due to dissolution weakens the shells as indicated by biomechanical tests (Barclay et al., 2020). Gaylord et al. (2011) indicated that the functional decline in shell integrity and strength of *M. californianus* under low pH, might not be the result of reductions in calcification and shell thickness but could be provoked by changes in shell architecture or material properties.

Ocean warming and acidification have been proven to affect physiological responses in marine molluscs (e.g., depression of metabolic rate, Bibby et al., 2007; alterations of immune responses and enzyme production, Matozzo et al., 2013), as well as behavioral responses related to predator avoidance (Bibby et al., 2007), reduction of feeding efficiency (Vargas et al., 2013) and movement restriction (Ellis et al., 2009). *Hexaplex trunculus* was less successful in reaching their food source under low pH (Chatzinikolaou et al., 2019). If such physiological and behavioral restrictions already deteriorate the ability of organisms to successfully cope with predation pressure, a thinner shell will certainly make the situation less favorable. The normally occurring shell thickening of *Littorina littorea* in the presence of predatory crabs was prohibited under low pH conditions, therefore limiting the morphological defense mechanisms in this species and threatening its survival (Bibby et al., 2007). *Austrocochlea porcata* exhibited depressed shell repair rate and compromised shell integrity under lower than ambient pH (pH = 7.7), both representing critical attributes for survival and protection against predators (Coleman et al., 2014). Molluscs under ocean acidification may display complex patterns of energy allocation toward predatory defense, as well as alterations in chemoreception, cue detection and predator avoidance behavior that may influence predator-prey interactions (Kroeker et al., 2014). If atmospheric CO<sub>2</sub> levels continue to rise and ocean pH to subsequently drops, less resistant species may face increased predation pressure and competition in comparison to more successful taxa within the same community, thus altering the balance within intertidal communities (Coleman et al., 2014).

## REFERENCES

- Andersson, A. J., Mackenzie, F. T., and Lerman, A. (2006). Coastal ocean CO<sub>2</sub>—carbonic acid—carbonate sediment system of the Anthropocene. *Glob. Biogeochem. Cycles* 20:GB1S92.
- Barclay, K. M., Gaylord, B., Jellison, B. M., Shukla, P., Sanford, E., and Leighton, L. R. (2019). Variation in the effects of ocean acidification on shell growth and strength in two intertidal gastropods. *Mar. Ecol. Prog. Ser.* 626, 109–121. doi: 10.3354/meps13056

Nevertheless, the effects of ocean acidification in the natural environment are subject to ecological and evolutionary processes, since marine calcifiers have demonstrated a remarkable degree of adaptation in a future high-CO<sub>2</sub> world being able to adapt and produce durable shells (Leung et al., 2020). Further investigation of species or shell region specific adaptation mechanisms could enlighten the potential plasticity of shell building organisms to acclimate to a continuously changing marine environment.

## DATA AVAILABILITY STATEMENT

The raw data supporting the conclusions of this article will be made available by the authors, without undue reservation.

## AUTHOR CONTRIBUTIONS

EC designed the research, participated in the experiment, scanned the samples, analyzed the images, performed the statistical analysis and wrote the manuscript. KK participated in the experiment, scanned the samples, analyzed the images. PG participated in the experiment, participated in the statistical analysis. All authors contributed to the article and approved the submitted version.

## FUNDING

The study was funded under the projects ECCO (HFRI, Hellenic Foundation for Research and Innovation for the support of Post-doctoral Researchers, project ID 343) and MOUNT – Modern unifying trends in marine biology (NSRF - MIS 5002470).

## ACKNOWLEDGMENTS

The authors would like to thank CretAquarium for providing the experimental tanks and the project BIOIMAGING-GR (NSFR - MIS 5002755) for offering expertise on scanning protocols and workflows.

## SUPPLEMENTARY MATERIAL

The Supplementary Material for this article can be found online at: <https://www.frontiersin.org/articles/10.3389/fmars.2021.645660/full#supplementary-material>

- Barclay, K. M., Gingras, M. K., Packer, S. T., and Leighton, L. R. (2020). The role of gastropod shell composition and microstructure in resisting dissolution caused by ocean acidification. *Mar. Environ. Res.* 162:105105. doi: 10.1016/j.marenvres.2020.105105
- Barroso, C. M., Moreira, M. H., and Richardson, C. A. (2005). Age and growth of *Nassarius reticulatus* in the ria de aveiro, north-west Portugal. *J. Mar. Biol. Assoc. U.K.* 85, 151–156. doi: 10.1017/s0025315405010970h
- Bibby, R., Cleall-Harding, P., Rundle, S., Widdicombe, S., and Spicer, J. (2007). Ocean acidification disrupts induced defences in the intertidal

- gastropod *Littorina littorea*. *Biol. Lett.* 3, 699–701. doi: 10.1098/rsbl.2007.0457
- Bouillon, J. (1958). Quelques observations sur la nature de la coquille chez les mollusques. *Ann. Soc. R. Zool. Malacol. Belg.* 89, 229–237.
- Byrne, M., and Fitzer, S. (2019). The impact of environmental acidification on the microstructure and mechanical integrity of marine invertebrate skeletons. *Conserv. Physiol.* 7:coz062.
- Cespuglio, G., Piccinetti, C., and Longinelli, A. (1999). Oxygen and carbon isotope profiles from *Nassa mutabilis* shells (*Gastropoda*): accretion rates and biological behaviour. *Mar. Biol.* 135, 627–634. doi: 10.1007/s002270050663
- Chatzinikolaou, E., Grigoriou, P., Keklikoglou, K., Faulwetter, S., and Papageorgiou, N. (2017). The combined effects of reduced pH and elevated temperature on the shell density of two gastropod species measured using micro-CT imaging. *ICES J. Mar. Sci.* 74, 1135–1149. doi: 10.1093/icesjms/fsw219
- Chatzinikolaou, E., Grigoriou, P., Martini, E., and Steriotti, A. (2019). Impact of ocean acidification and warming on the feeding behaviour of two gastropod species. *Mediterr. Mar. Sci.* 20, 669–679. doi: 10.12681/mms.19187
- Chatzinikolaou, E., and Richardson, C. A. (2008). Population dynamics and growth of *Nassarius reticulatus* (*Gastropoda: Nassariidae*) in Rhosneigr (Anglesey, UK). *Mar. Biol.* 153, 605–619. doi: 10.1007/s00227-007-0835-5
- Coleman, D. W., Byrne, M., and Davis, A. R. (2014). Molluscs on acid: gastropod shell repair and strength in acidifying oceans. *Mar. Ecol. Prog. Ser.* 509, 203–211. doi: 10.3354/meps10887
- Cross, E., Harper, E. M., and Peck, L. S. (2019). Thicker shells compensate extensive dissolution in brachiopods under future ocean acidification. *Environ. Sci. Technol.* 53, 5016–5026. doi: 10.1021/acs.est.9b00714
- DeCarlo, T. M., Comeau, S., Cornwall, C. E., and McCulloch, M. T. (2018). Coral resistance to ocean acidification linked to increased calcium at the site of calcification. *Proc. R. Soc. B.* 285:20180564. doi: 10.1098/rspb.2018.0564
- Delamotte, M., and Vardala-Theodorou, E. (2007). *Shells from the Greek Seas*. Athens: Goulandri Natural History Museum, 330.
- Dickson, A. G., and Millero, F. J. (1987). A comparison of the equilibrium constants for the dissociation of carbonic acid in seawater media. *Deep Sea Res. A* 34, 1733–1743. doi: 10.1016/0198-0149(87)90021-5
- Dickson, A. G., Sabine, C. L., and Christian, J. R. (2007). Guide to best practices for ocean CO<sub>2</sub> measurements. *PICES Special Publication* 3, 1–191.
- Doney, S. C., Busch, D. S., Cooley, S. R., and Kroeker, K. J. (2020). The impacts of ocean acidification on marine ecosystems and reliant human communities. *Annu. Rev. Environ. Resour.* 45, 11.1–11.30.
- Doney, S. C., Fabry, V. J., Feely, R. A., and Kleypas, J. A. (2009). Ocean acidification: the other CO<sub>2</sub> problem. *Annu. Revis. Mar. Sci.* 1, 169–192.
- Ellis, R. P., Bersey, J., Rundle, S. D., Hall-Spencer, J. M., and Spicer, J. I. (2009). Subtle but significant effects of CO<sub>2</sub> acidified seawater on embryos of the intertidal snail, *Littorina obtusata*. *Aquat. Biol.* 5, 41–48. doi: 10.3354/ab00118
- Eriksson, S., and Tallmark, B. (1974). The influence of environmental factors on the diurnal rhythm of the prosobranch gastropod *Nassarius reticulatus* (L.) from a non-tidal area. *Zoon* 2, 135–142.
- Feely, R. A., Sabine, C. L., Lee, K., Berelson, W., Kleypas, J., Fabry, J., et al. (2004). Impact of anthropogenic CO<sub>2</sub> on the CaCO<sub>3</sub> system in the oceans. *Science*. 305, 362–366. doi: 10.1126/science.1097329
- Fisher, J. A. D., Rhile, E. C., Liu, H., and Petraitis, P. S. (2009). An intertidal snail shows a dramatic size increase over the past century. *Proc. Natl. Acad. Sci. U.S.A.* 106, 5209–5212. doi: 10.1073/pnas.0812137106
- Fitzer, S. C., Vittert, L., Bowman, A., Kamenos, N. A., Phoenix, V. R., and Cusack, M. (2015). Ocean acidification and temperature increase impact mussel shell shape and thickness: problematic for protection? *Ecol. Evol.* 5, 4875–4884. doi: 10.1002/ece3.1756
- Foster, P., and Cravo, A. (2003). Minor elements and trace metals in the shell of marine gastropods from a shore to tropical East Africa. *Water Air Soil Pollut.* 145, 53–65.
- Gaylord, B., Hill, T. M., Sanford, E., Lenz, E. A., Jacobs, L. A., Sato, K. N., et al. (2011). Functional impacts of ocean acidification in an ecologically critical foundation species. *J. Exp. Biol.* 214, 2586–2594. doi: 10.1242/jeb.055939
- Gazeau, F., Parker, L. M., Comeau, S., Gattuso, J. P., O'Connor, W. A., Martin, S., et al. (2013). Impacts of ocean acidification on marine shelled molluscs. *Mar. Biol.* 160, 2207–2245. doi: 10.1007/s00227-013-2219-3
- Gizzi, F., Caccia, M. G., Simoncini, G. A., Mancuso, A., Reggi, M., Fermani, S., et al. (2016). Shell properties of commercial clam *Chamelea gallina* are influenced by temperature and solar radiation along a wide latitudinal gradient. *Sci. Rep.* 6:36420.
- Harris, K. E., DeGrandpre, M. D., and Hales, B. (2013). Aragonite saturation state dynamics in a coastal upwelling zone. *Geophys. Res. Lett.* 40, 2720–2725. doi: 10.1002/grl.50460
- Harvey, B. P., Agostini, S., Wada, S., Inaba, K., and Hall-Spencer, J. M. (2018). Dissolution: the achilles' heel of the triton shell in an acidifying Ocean. *Front. Mar. Sci.* 5:371. doi: 10.3389/fmars.2018.00371
- Hildebrand, T., and Rügsegger, P. (1997). A new method for the model-independent assessment of thickness in three-dimensional images. *J. Microsc.* 185, 67–75. doi: 10.1046/j.1365-2818.1997.1340694.x
- Hughes, R. N. (1986). *A Functional Biology of Marine Gastropods*. London: Croom Helm Ltd, 245.
- IPCC (2014). “Climate change 2014: synthesis report,” in *Contribution of Working Groups I, II and III to the 5th Assessment Report of the Intergovernmental Panel on Climate Change*, eds R. K. Pachauri and L. A. Meyer (Geneva: IPCC), 151.
- Kleypas, J. A., Feely, R. A., Fabry, V. J., Langdon, C., and Sabine, C. L. (2006). *Impacts of Ocean Acidification on Coral Reefs and Other Marine Calcifiers: A Guide to Future Research*. Report of a workshop held 18–20 April 2005, St. Petersburg, FL, sponsored by NSF, NOAA, and the US Geological Survey. Contribution No. 2897. Seattle, WA: NOAA.
- Kroeker, K. J., Sanford, E., Jellison, B. M., and Gaylord, B. (2014). Predicting the effects of ocean acidification on predator-prey interactions: a conceptual framework based on coastal molluscs. *Biol. Bull.* 226, 211–222. doi: 10.1086/bblv226n3p211
- Langer, G., Nehrke, G., Baggini, C., Rodolfo-Metalpa, R., Hall-Spencer, J. M., and Bijma, J. (2014). Limpets counteract ocean acidification induced shell corrosion by thickening of aragonitic shell layers. *Biogeosciences* 11, 7363–7368. doi: 10.5194/bg-11-7363-2014
- Leung, J. Y. S., Chen, Y., Nagelkerken, I., Zhang, S., Xie, Z., and Connell, S. D. (2020). Calcifiers can adjust shell building at the nanoscale to resist ocean acidification. *Small* 16:2003186. doi: 10.1002/sml.202003186
- Leung, J. Y. S., Connell, S. D., Nagelkerken, I., and Russell, B. D. (2017a). Impacts of near-future ocean acidification and warming on the shell mechanical and geochemical properties of gastropods from intertidal to subtidal zones. *Environ. Sci. Technol.* 51, 12097–12103. doi: 10.1021/acs.est.7b02359
- Leung, J. Y. S., Russell, B. D., and Connell, S. D. (2017b). Mineralogical plasticity acts as a compensatory mechanism to the impacts of ocean acidification. *Environ. Sci. Technol.* 51, 2652–2659. doi: 10.1021/acs.est.6b04709
- Li, S., Huang, J., Liu, C., Liu, Y., Zheng, G., Xie, L., et al. (2016). Interactive effects of seawater acidification and elevated temperature on the transcriptome and biomineralization in the pearl oyster *Pinctada fucata*. *Environ. Sci. Technol.* 50, 1157–1165. doi: 10.1021/acs.est.5b05107
- Marshall, D. J., Abdelhady, A. A., Wah, D. T. T., Mustapha, N., Gödeke, S. H., De Silva, L. C., et al. (2019). Biomonitoring acidification using marine gastropods. *Sci. Total Environ.* 692, 833–843. doi: 10.1016/j.scitotenv.2019.07.041
- Matozzo, V., Chinellato, A., Munari, M., Bressan, M., and Marin, M. G. (2013). Can the combination of decreased pH and increased temperature values induce oxidative stress in the clam *Chamelea gallina* and the mussel *Mytilus galloprovincialis*? *Mar. Pollut. Bull.* 72, 34–40. doi: 10.1016/j.marpolbul.2013.05.004
- Mehrbach, C., Culberson, C. H., Hawley, J. E., and Pytkowicz, R. M. (1973). Measurement of the apparent dissociation constants of carbonic acid in seawater at atmospheric pressure. *Limnol. Oceanogr.* 18, 897–907. doi: 10.4319/lo.1973.18.6.0897
- Melatunan, S., Calosi, P., Rundle, S. D., Widdicombe, S., and Moody, A. J. (2013). Effects of ocean acidification and elevated temperature on shell plasticity and its energetic basis in an intertidal gastropod. *Mar. Ecol. Prog. Ser.* 472, 155–168. doi: 10.3354/meps10046
- Morton, B., and Chan, K. (2004). The population dynamics of *Nassarius festivus* (*Gastropoda: Nassariidae*) on three environmentally different beaches in Hong Kong. *J. Mollusc. Stud.* 70, 329–339. doi: 10.1093/mollusc/70.4.329
- Nehrke, G., Poigner, H., Wilhelms-Dick, D., Brey, T., and Abele, D. (2012). Coexistence of three calcium carbonate polymorphs in the shell of the Antarctic clam *Laternula elliptica*. *Geochem. Geophys. Geosyst.* 13:Q05014.

- Nienhuis, S., Palmer, A. R., and Harley, C. D. G. (2010). Elevated CO<sub>2</sub> affects shell dissolution rate but not calcification rate in a marine snail. *Proc. R. Soc. B Biol. Sci.* 277, 2553–2558. doi: 10.1098/rspb.2010.0206
- Orr, J. C., Fabry, V. J., Aumont, O., Bopp, L., Doney, S. C., Feely, R. A., et al. (2005). Anthropogenic ocean acidification over the twenty-first century and its impact on calcifying organisms. *Nature* 437, 681–686. doi: 10.1038/nature04095
- Queirós, A. M., Fernandes, J. A., Faulwetter, S., Nunes, J., Rastrick, S. P. S., Mieszkowska, N., et al. (2015). Scaling up experimental ocean acidification and warming research: from individuals to the ecosystem. *Glob. Change Biol.* 21, 130–143. doi: 10.1111/gcb.12675
- Reindl, S., and Haszprunar, G. (1994). Light and electron microscopical investigations on shell pores (caeca) of fissurellid limpets (*Mollusca: Archaeogastropoda*). *J. Zool.* 233, 385–404. doi: 10.1111/j.1469-7998.1994.tb05272.x
- Ries, J. B., Cohen, A. L., and McCorkle, D. C. (2009). Marine calcifiers exhibit mixed responses to CO<sub>2</sub>-induced ocean acidification. *Geology*. 37, 1131–1134. doi: 10.1130/g30210a.1
- Ruppert, E. E., and Barnes, R. D. (1996). *Invertebrate Zoology*. Philadelphia, PA: Saunders College Publishing, 1055.
- Shirayama, Y., and Thornton, H. (2005). Effect of increased atmospheric CO<sub>2</sub> on shallow water marine benthos. *J. Geophys. Res.* 110:C09S08.
- Starmühlner, F. (1969). Zur molluskenfauna des felslitorals bei rovinj (Istrien). *Malacologia* 9, 217–242.
- Taylor, J. D. (1987). Feeding ecology of some common intertidal neogastropods at Djerba, Tunisia. *Vie Milieu* 37, 13–20.
- Vargas, C. A., de la Hoz, M., Aguilera, V., San Martin, V., Manríquez, P. H., Navarro, J. M., et al. (2013). CO<sub>2</sub>-driven ocean acidification reduces larval feeding efficiency and changes the food selectivity in the mollusk *Concholepas concholepas*. *J. Plankton Res.* 35, 1059–1068. doi: 10.1093/plankt/fbt045
- Wahl, M., Saderne, V., and Sawall, Y. (2016). How good are we at assessing the impact of ocean acidification in coastal systems? Limitations, omissions and strengths of commonly used experimental approaches with special emphasis on the neglected role of fluctuations. *Mar. Freshw. Res.* 67, 25–36. doi: 10.1071/mf14154
- Zhang, H., Shin, P. K. S., and Cheung, S. G. (2016). Physiological responses and scope for growth in a marine scavenging gastropod, *Nassarius festivus* (Powys, 1835), are affected by salinity and temperature but not by ocean acidification. *ICES J. Mar. Sci.* 73, 814–824. doi: 10.1093/icesjms/fsv208

**Conflict of Interest:** The authors declare that the research was conducted in the absence of any commercial or financial relationships that could be construed as a potential conflict of interest.

Copyright © 2021 Chatzinikolaou, Keklikoglou and Grigoriou. This is an open-access article distributed under the terms of the Creative Commons Attribution License (CC BY). The use, distribution or reproduction in other forums is permitted, provided the original author(s) and the copyright owner(s) are credited and that the original publication in this journal is cited, in accordance with accepted academic practice. No use, distribution or reproduction is permitted which does not comply with these terms.